

Flocs as vectors for microplastics in the aquatic environment

Received: 12 July 2023

Accepted: 1 October 2024

Published online: 8 November 2024

 Check for updatesNan Wu¹✉, Stuart W. D. Grieve^{1,2}, Andrew J. Manning^{3,4} & Kate L. Spencer¹

Microplastics (MPs) are an important component of suspended particulate matter in aquatic environments with two main transport modes, that is, as individual entities or in flocs. Despite its importance to MP pollution management, understanding and predicting MP flocculation remains a challenge. In this Article, we combined a meta-analysis of published data (>2,000 measurements) with new experimental data (>4,000 measurements) to investigate which size fraction of MPs can be incorporated into and transported by flocs in the aquatic environment. The size relationship between MPs and flocs can be used to predict the flocculation of MPs in various aquatic environments, and we have proposed a mathematical model to show that small MPs (<162 μm) are predominantly transported as flocs, regardless of the physicochemical characteristics of the MPs or water body. This provides valuable information to predict the transport modes of MPs, presenting a critical insight for multiple environmental settings and future pollution control strategies.

Microplastics (MPs, plastic particles < 5 mm) are increasingly considered an important component of suspended particulate matter (SPM) pools in various aquatic environments due to the continuous input of MPs^{1–4}. Flocculation is a fundamental process in the aquatic environment that controls the fate of SPM (including MPs), whereby fine particles are aggregated into large aggregates or ‘flocs’ (Fig. 1a, aggregation processes), enhancing the sedimentation of incorporated primary particles (including MPs)^{5,6}. The resultant flocs are loose, irregular, highly porous aggregates of minerogenic and biogenic material with the probability of break-up increasing with size (Fig. 1a, breakage processes)^{5,7}. Flocculation is a critical process that controls fine sediment transport in fluvial systems⁵, vertical carbon flux in the ocean⁸, and water quality and nutrient cycling in lakes and reservoirs⁹ (Fig. 1b).

Once MPs are incorporated into flocs (Fig. 1a,c), their transport reflects the hydrodynamic behaviour of the floc, including its horizontal movement¹⁰, vertical settling¹¹ and resuspension^{12,13} at multiple temporal and spatial scales (Fig. 1b). As such, buoyant MPs may settle with flocs and the overall settling velocity of non-buoyant MPs will increase¹¹, enhancing the vertical depositional transport flux of MPs and thus their removal from the water column. Thus, flocculation is a critical

process that promotes the natural removal of MPs from the ocean surface^{14–16}, contributes to both temporary and permanent sinks of MPs in freshwater environments such as rivers, lakes and reservoirs^{10,12,17}, reduces the river-to-sea flux of MPs in estuarine environments¹⁸, and influences the removal efficiency of MPs in coagulation and flocculation in engineered¹⁹ water environments (Fig. 1b). Many modelling studies attempt to predict the fate and impact of MPs, but they either ignore the importance of flocculation (by generally assuming that all MPs are transported as individual inert particles^{20,21}) or use inappropriate parameters to characterize the flocculation of MPs (for example, they assume that all MPs can be incorporated into flocs) to predict their fate and functioning within aquatic environments^{17,22,23}. Consequently, a comprehensive understanding of the flocculation of MPs is a fundamental and essential requirement to rigorously model the fate and impact of MPs in both transport modes in aquatic environments.

For over a decade, many studies have investigated the influence of the various parameters that contribute to the flocculation of MPs, yet understanding and quantifying this process remains elusive^{2,24}. This is because MPs vary in size across six orders of magnitude and exhibit wide-ranging physical (for example, shape, density and surface

¹School of Geography, Queen Mary University of London, London, UK. ²Digital Environment Research Institute, Queen Mary University of London, London, UK. ³HR Wallingford, Wallingford, Oxfordshire, UK. ⁴School of Biological and Marine Sciences, University of Plymouth, Plymouth, UK.

✉e-mail: n.wu@qmul.ac.uk

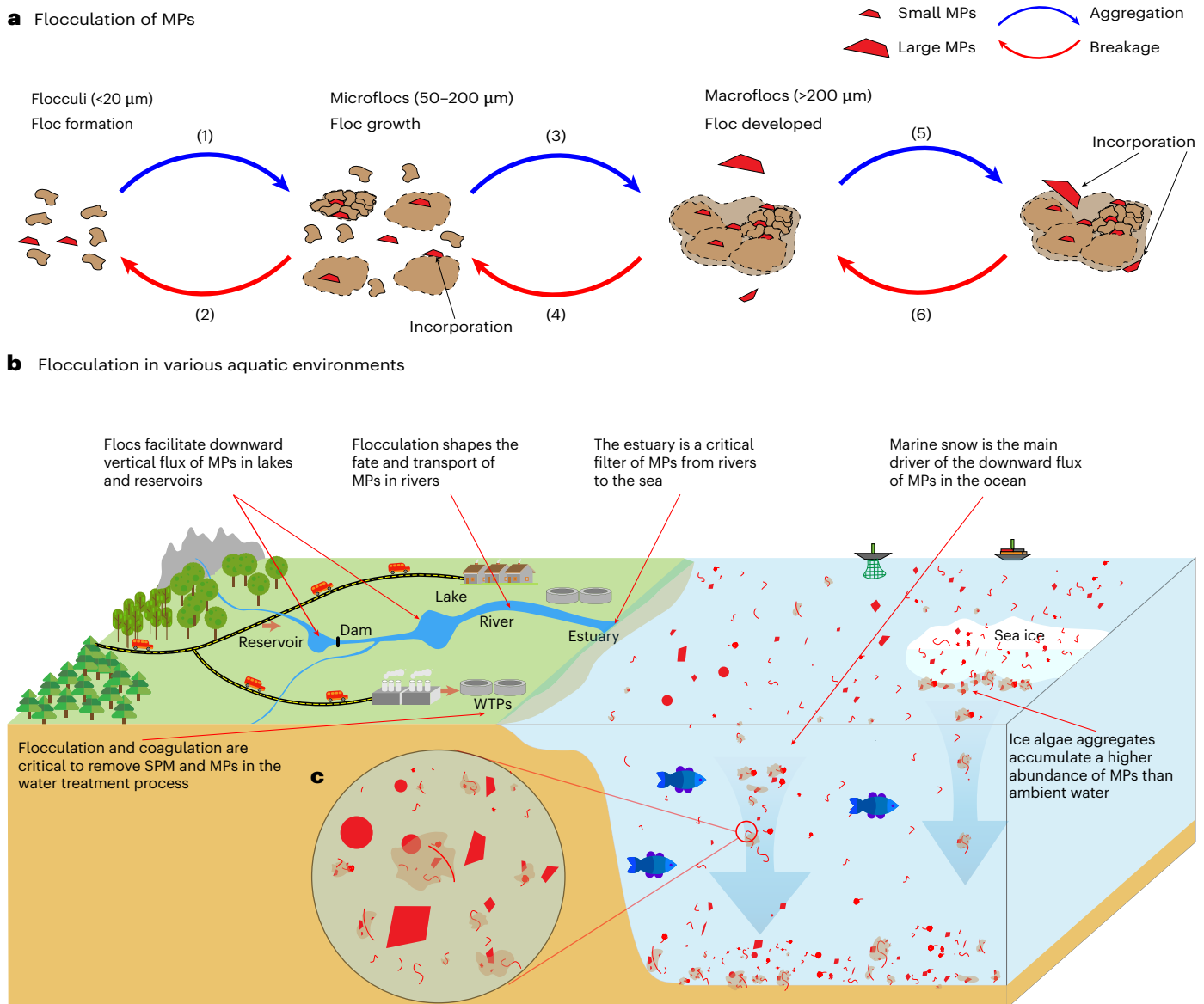


Fig. 1 | Influence of flocculation on the fate and impact of MPs in various aquatic environments. **a**, The flocculation of fine particles aggregating into large flocs and the disaggregation of large flocs into small flocs and individual particles. Flocculi ($<20\ \mu\text{m}$) are the building blocks of flocs. Brown particles, flocs; red particles, MPs. **b**, Incorporation of MPs (red particles, microspheres and fragments; threads, microfibres) with different properties into flocs (brown

particles) in multiple aquatic environments, including rivers, reservoirs, lakes, estuaries, marine environments, sea ice and water treatment plants (WTPs). **c**, Incorporation dynamics of MPs: while some MPs can be incorporated into flocs, not all sizes of MP are suitable for incorporation. Those MPs that do get incorporated are then transported along with flocs.

morphology) and chemical (for example, polymer type, hydrophobicity, surface charge and ageing condition) properties^{2,21}. MPs have been documented in all aquatic ecosystems with highly variable chemical and hydrodynamic conditions, and the composition and concentration of the flocs with which they associate are also diverse^{5,9,11,18,19} (Fig. 1a). Hence, the rates and mechanisms by which MPs are incorporated into flocs are, in all probability, likely to be highly variable and this presents a major challenge when predicting their transport behaviours.

Therefore, our overarching aim is to understand how MPs flocculate, specifically, which MP size fractions can be incorporated into flocs in various aquatic environments. Hence, in this Article, we (1) examined the flocculation of MPs with flocs from differing aquatic conditions (derived from 2,580 data measurements) by means of a meta-analysis and (2) conducted a series of flocculation experiments to quantify the influence of MP properties on their flocculation behaviours. The results of this study will have the potential to lead to considerable advances

in the development of empirical mathematical models to predict the transport modes of MPs (that is, transported individually or as part of flocs) in various aquatic environments.

Meta-analysis of the size relationship between MPs and flocs

The meta-dataset comprised 2,580 measurements of MPs and flocs, predominantly derived from laboratory experiments (Fig. 2a), including floc sizes ranging from $10\ \mu\text{m}$ (the typical lower size limit of flocs in natural and engineered water^{5,7}) to a few millimetres (macro- and megaflocs) and various experimental parameters (for example, salinity, turbulence, pH, temperature, organic matter component, SPM composition and concentration) that represent wide-ranging aquatic environments (for example, marine, estuary, freshwater and engineered water; Fig. 2a,b). The MPs observed ranged from $100\ \text{nm}$ to $5\ \text{mm}$ and included wide-ranging polymer types (Fig. 2c). Hence, the meta-dataset

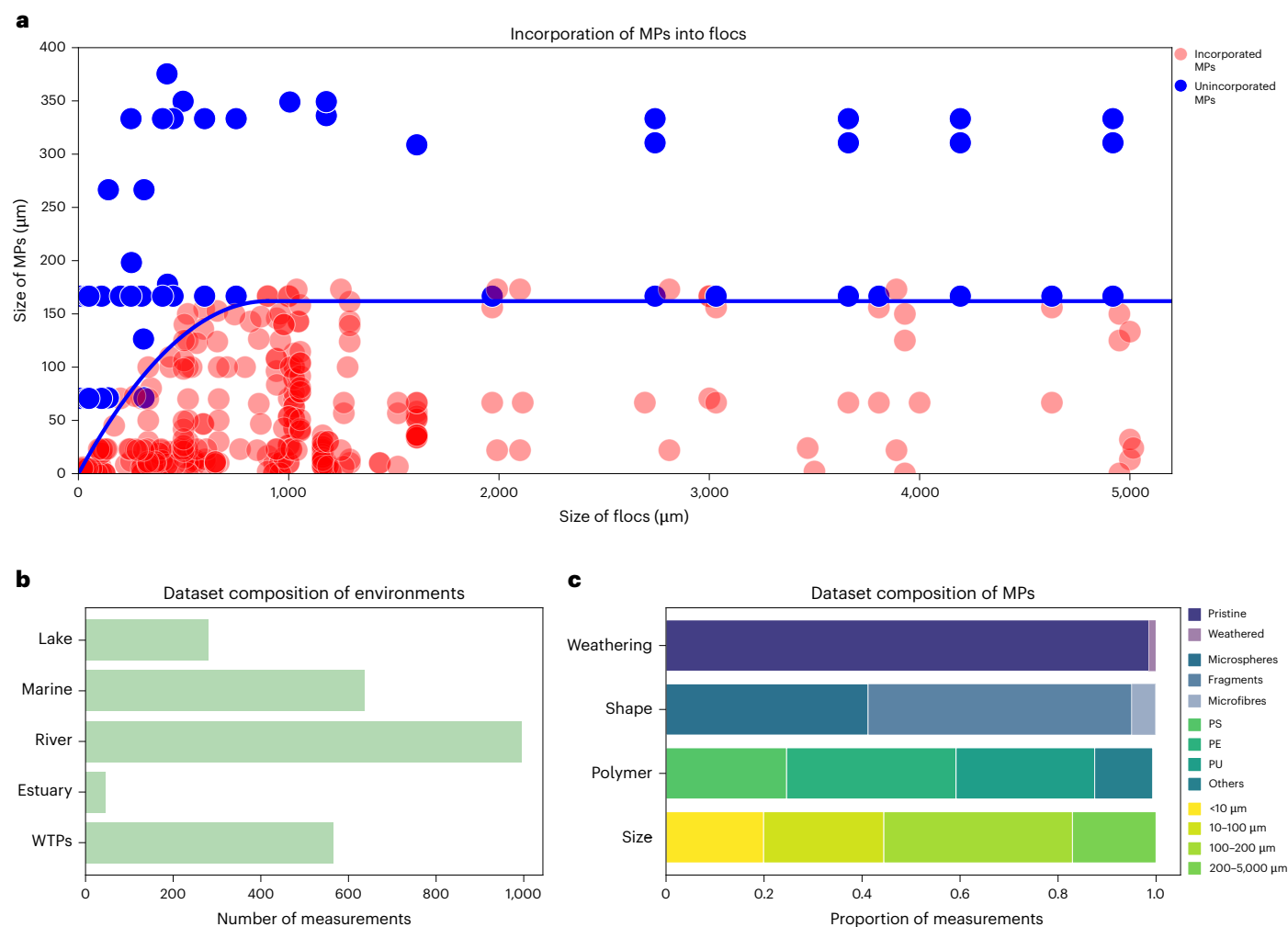


Fig. 2 | Meta-analysis of the size relationship between MPs and hosting flocs.

a, The meta-analysis for the incorporation of MPs into flocs as a function of size, showing MPs incorporated into flocs (red dots) and unincorporated MPs (blue dots). A boundary curve is fitted to differentiate the MPs into two groups: those that are incorporated into flocs fall under the curve (red dots) and those that are unincorporated lie above the curve (blue dots), with 95.4% of incorporated MPs under the curve. The scatter plot is based on 2,580 measurements and comprises

394 data dots. **b**, The meta-dataset composition of the environments of flocs based on the number of measurements. **c**, The meta-dataset composition of the MPs based on the proportion of measurements. Here, MP size (μm) is the smallest dimension: diameter for microspheres, diameter for microfibres and minimum Feret diameter for irregular-shaped fragments. PS, polystyrene; PE, polyethylene; PU, polyurethane.

represents a full spectrum of aquatic environmental conditions and floc size, as well as MP size and polymer type.

We explored the relationship between MP size and floc size, and even with remarkably high complexities in both the MPs and experimental conditions, there is a clearly defined boundary curve (equation (1)) that differentiates MPs that are incorporated into, and hence transported by flocs (MP_{floc} ; under the curve) and MPs that are not incorporated into flocs ($\text{MP}_{\text{non-floc}}$; above the curve) and thus transported as individual particles (Fig. 2a). Over 95% of MP_{floc} are below the boundary curve:

$$\begin{aligned} x \leq 900\ \mu\text{m}, y &= -0.0002x^2 + 0.36x \\ x > 900\ \mu\text{m}, y &= 162 \end{aligned} \quad (1)$$

where x represents the size of flocs (μm) and y represents the size of MPs (μm ; measured along the shortest dimension).

This is the first study to predict the transport mode of MPs by simply considering floc size, addressing a gap in previous research that has solely focused on how environmental properties such as salinity, turbulence, pH, and the composition and concentration of SPM may

influence MP flocculation. Low turbulence^{11,13,18}, high concentrations of organic matter or biofloculants^{19,25}, and high ion concentrations (for example, high salinity)^{10,26} enhance the interaction and incorporation of MPs into flocs. While previous studies have described these environmental effects, they have been unable to provide predictive capabilities for MP flocculation across different environments². Our findings demonstrate that these parameters uniformly affect floc size, which in turn is a meta-control on their capacity to incorporate MPs. This understanding has led us to identify floc size as a critical and effective predictor for the flocculation of MPs, as depicted in Fig. 2a. Thus, floc size emerges as a pivotal parameter, reflecting the environmental conditions conducive to MP incorporation and enhancing our ability to predict MP behaviour in various aquatic settings.

Whilst the meta-dataset covers a wide range of MP sizes and environmental conditions, over 90% of the studies from which the data derive used pristine microspheres and fragments, which is not representative of the diversity of MPs typically found in the natural environment (Fig. 2c)^{2,27}. A large amount of the data stem from single MP sizes and single floc sizes, reflecting a gap in the literature where the size relationship between MPs and flocs is not a primary research objective^{11,12,19,24,26}. More importantly, previous studies only focused

on one measure of size, namely, the longest dimension. These gaps highlight the need to study a wide range of MPs with different sizes and properties, alongside a continuous spectrum of floc sizes. This work aimed to bridge the identified knowledge gaps and enhance the predictability and accuracy of MP flocculation models, ultimately contributing to a more robust understanding of MP distribution and behaviour in various aquatic environments.

Experiments on the size relationship between MPs and flocs

A series of laboratory experiments using a continuous size range of MPs with different signature shapes (that is, fragments, microfibrils and microspheres), eight polymer types, three density ranges and weathered versus pristine states were conducted to examine how the properties of MPs influenced their incorporation into flocs with a continuous size range of 10–1,100 μm (Methods and Supplementary Tables 1 and 2). The sizes of the flocs and incorporated MPs from this experimental dataset were then plotted with >99.0% (1,894/1,913 for microspheres and fragments and 2,202/2,204 for microfibrils; Supplementary Fig. 1) of MP_{floc} plotting under the boundary curve derived from the meta-analysis (Fig. 3a). Moreover, the incorporation rate (the ratio between the incorporated MPs and total MPs; Fig. 3a) is also aligned with the boundary curve. The incorporation rate decreases as the size of the MPs increases, starting at 97.0% for MPs smaller than 20 μm and dropping to 9.7% for MPs larger than 162 μm (upper boundary of the boundary curve, Figs. 2a and 3a). This indicates that the large MPs above the boundary curve are rarely incorporated into flocs up to a size of 1,100 μm . Therefore, both our experimental data and the data from the meta-analysis can be predicted based on the size relationship between flocs and MPs, and the boundary curve can be used to predict the flocculation behaviours of MPs in various aquatic environments.

The boundary curve

The boundary curve can be divided into three distinct zones (Figs. 2a and 3a). In Zone 1 (MPs < 63 μm and flocs < 200 μm), the curve is nearly linear. Flocs are frequently described as having scale-dependent or ‘fractal’ aggregation hierarchies⁶ and hence the maximum size of a particle that can be incorporated into an existing floc is proportional to the floc size^{28–30}. The flocs in Zone 1 broadly coincide with the smallest floc units, namely, ‘floculi’ (<20 μm) and ‘microflocs’ (<200 μm), defined in the literature^{7,31} (Fig. 1a). Aggregation mechanisms are dominated by electroflocculation and polymer-bridging, forming stable, dense flocs with micrometre-scale intra-aggregate porosity^{7,31,32}. Turbulence-led disaggregation of MPs is linearly linked to their area and resistance to hydrodynamic force, which is not strong enough to detach small MPs (<63 μm) from flocs. Here, aggregation is the dominant mechanism by which MPs are incorporated into flocs, with the size ratio between MPs and flocs (0.36, equation (1)) being the key limitation for MP flocculation. This is consistent with both the results of the meta-analysis and our laboratory experiments.

With increasing MP size (>63 μm), the nonlinearity of the boundary curve in Zone 2 (flocs from 200 μm to 900 μm) implies that the mechanisms by which MPs are incorporated into flocs are no longer linear scale-dependent. These larger ‘macroflocs’ (sometimes defined as flocs, with a size > 200 μm)^{25,33} are critical to the mass settling sediment flux (and also by implication to the MP settling flux) in aquatic environments and are characterized by highly porous and irregular structures, with bioflocculation and the extracellular polymeric substance (EPS) bridging effect playing an increasingly important role in aggregation^{7,25}. Here, the shear plane between MPs and flocs increases with increasing size of the MPs on account of the hydrodynamic force difference between the impermeable MPs and permeable flocs^{28,29}. This increases the likelihood of the detachment of MPs (Fig. 1a, routes 6 and 4) and reduces both the flocculation efficiency and the maximum size range of MPs that can be incorporated into flocs. The slope between

the maximum size of MPs and floc size decreases with MP size, reaching 0 for MPs > 162 μm ; this zone demonstrates the influence of hydrodynamic turbulent forces contributing towards a continuous process of aggregation and break-up, resulting in a dynamic quasi-equilibrium controlled by their particle bonding strength and floc size within a given shear field, typically as defined by the Kolmogorov microscale³⁴.

For the meta-analysis, the boundary curve (Zone 3) plateaus for MPs > 162 μm . For the experimental data, the incorporation rate for MPs > 162 μm is extremely low at 9.7%, even for very large flocs (>1,100 μm ; Fig. 3a and Supplementary Data 2), which means that MPs > 162 μm are highly unlikely to be incorporated. The incorporation rate of the experimental data aligns with the boundary curve. In Zone 3, we have ‘megaflocs’ (>900 μm)⁷, which are associations of macroflocs held together very loosely by biopolymer backbone and anchoring mechanisms often with millimetre-scale porosity^{7,25}. Here, the mechanisms leading to aggregation between MPs and flocs are not stable, even for flocs in excess of 3,000 (ref. 12). This is due to the shear plane between MPs and flocs always surpassing the relatively weak cohesive forces and compelling MPs to detach from the floc structure³⁰. This part of the boundary curve is predominantly based on data from the meta-analysis as the experimental dataset is very limited when flocs are larger than 1,100 μm (Figs. 2a and 3a).

Environmental monitoring of MPs in flocs in the field is rare, but some recent studies also support our boundary curve. MPs detected in marine snow^{16,35,36} and algal aggregates under sea ice in the Arctic¹⁶ all fall under the boundary curve. Many studies have reported that small MPs (<100 μm) are correlated with SPM in the water column and sediment, but the same relationships have not been observed for large MPs (>200 μm)^{14,37–40}. However, we note that in some extreme situations with high concentrations of EPS or flocculant (for example, water treatment facilities), very large flocs (a few millimetres) can be produced and potentially this could lead to a high rate of incorporation of MPs larger than 162 μm (ref. 41). However, this is not representative of the natural aquatic environment^{16,35,36}.

Although not explored here and rarely observed in the natural environment, nanoplastics (that is, plastic particles < 100 nm) would fall below the boundary curve and be incorporated into flocs as flocs in natural and engineered waters⁵ are typically larger than 20 μm (ref. 26). Furthermore, as clay particles are commonly included in flocs and have an upper size boundary of 2 μm (refs. 5,29), nanoplastics, being considerably smaller, are also integrated into flocs without limitation.

Implications and significance of the boundary curve

The boundary curve can be used to predict the transport mode of MPs in various aquatic environments, aiding the prediction of the fate and transport of MPs separately for MP_{floc} and $\text{MP}_{\text{non-floc}}$ in the water environment. In particular, it can help in estuarine modelling to determine the river-to-sea flux of MPs and the rate of ocean deposition of small MPs. These insights are crucial to understand the missing budget of MPs in the ocean^{27,42}. Water treatment strategies can also be improved by strategically designing the removal of MPs that fall below the boundary curve through flocculation, making use of the MP size filter and other processes to prioritize $\text{MP}_{\text{non-floc}}$ removal processes for larger MPs.

Many studies have proposed that the association between MPs and SPM can influence the size, structure and transport of flocs, impacting biogeochemical cycling in various aquatic environments (Fig. 1b), including the biological carbon pump in oceans^{15,35,43}, nutrient cycling in lakes⁹, and the transport of fine sediment and organic matter within river deltas and estuaries¹⁸ (Fig. 1a). The accurate estimation of which size fraction of MPs associate with flocs is an important prerequisite to assess this influence. This boundary curve further implies that only MP_{floc} will have an effect on the structure, size and settling velocity of flocs across different aquatic environments. Therefore, a more accurate prediction of the influence of MPs on the ocean biological carbon

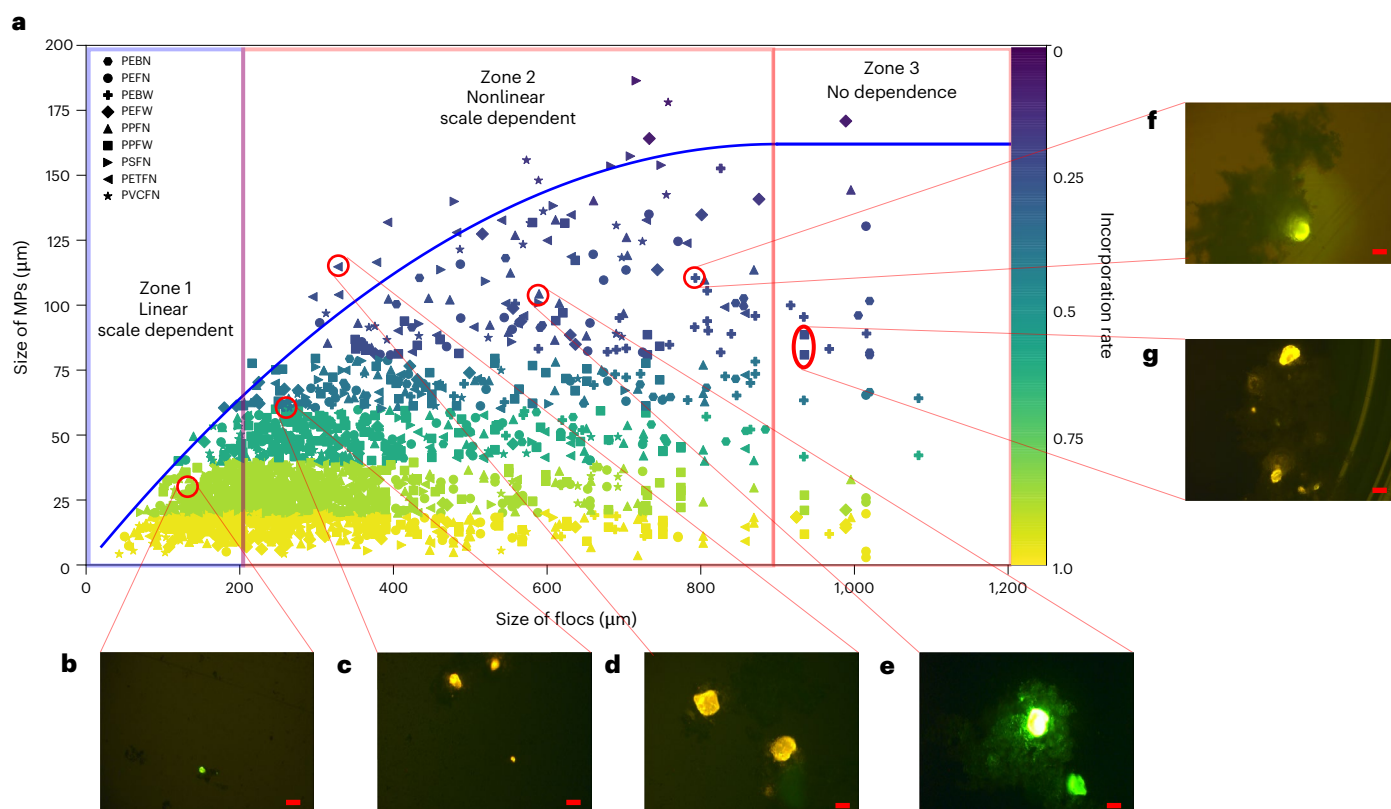


Fig. 3 | Experimental size relationship between MPs and hosting flocs. **a**, The relationship between incorporated MPs (fragments ($n = 1,804$) and microspheres ($n = 109$)) and flocs plotted as a function of size (x -axis range of 0–1,200 μm and y -axis range of 0–200 μm) and overlaid on the boundary curve based on the meta-analysis. The colours of the dots represent the incorporation rate of each type of MP (the ratio between the number of incorporated MPs and the total number of MPs was calculated for each type of MP in the flocculation experiment, see Methods); the incorporation rate decreases with increasing MP size. The boundary curve is divided into three zones: linear scale dependent, nonlinear scale dependent and no dependence. Eleven types of microfibre ($n = 2,204$)

with different diameters and lengths and distinct polymer types are illustrated in Supplementary Fig. 1. **b–g**, Examples of MP fragments and microspheres incorporated into flocs: PEFN (**b**), PETFN (**c**), PETFN (**d**), PPFN (**e**), PEBW (**f**) and PPFW (**g**). Scale bars in **b–g**, 100 μm . Each MP is represented by an abbreviation. The first two or three letters represent the type of polymer of the MP, namely, PE, PS, polypropylene (PP), polyethylene terephthalate (PET) and polyvinyl chloride (PVC). The next letter represents the shape of the MP: B represents microspheres and F represents fragments. The final letter is either N (non-weathered and pristine MP) or W (UV-weathered MP). Details of these MPs can also be found in Supplementary Tables 1 and 2.

pump, lake nutrient cycling, estuary and river sediment transport, and other SPM migrations in various aquatic environments can now be established (Fig. 1a).

The flocculation of MPs can also influence their ecological risk to organisms by changing exposure pathways. The redistribution of MPs through floc settling increases the bioavailability to subsurface and bottom-dwelling organisms^{11,15} and MP can be preferentially ingested by sediment- and detritus-feeding organisms^{35,44,45}. In some cases, flocs can also act as a shield to mitigate the toxicity of MPs and further influence ecological risk⁴⁶. This enhanced understanding of the fate and transport of MPs also informs our comprehension of their ecological risk. Consequently, the boundary curve can also be incorporated into the development of risk assessment frameworks for MPs.

Conclusions

The boundary curve, developed by integrating a large-scale meta-analysis with novel experimental data, unites flocculation theory with environmental observations across a range of aquatic environments. These results demonstrate that MP and floc interactions can be predicted via two simple and relatively easy-to-measure parameters: the size of MPs and the size of flocs in complex systems where the MPs are constantly changing (for example, through weathering and fragmentation) and the variability of the natural aquatic environment drives variability in floc formation.

The boundary curve model substantially enhances our understanding of the fate and behaviour of MPs in aquatic environments by providing a reliable method to predict whether MPs will be transported individually or as part of flocs. This development has broad implications, improving the modelling of MP fate and transport, optimizing MP removal from waste and raw water, and deepening our understanding of how flocculation affects ecological risks and biogeochemical impacts. Thus, this model not only advances our knowledge of MP dynamics but also supports more effective control and management of MP pollution across diverse aquatic settings.

Methods

Meta-analysis

Systematic review. Using the Web of Science, Scopus, Science Direct, PubMed and Google Scholar databases, we searched for papers on microplastic flocculation published between January 1907 (the year that Bakelite was developed⁴⁷) and November 2022. We used the following keywords and conditions in the searches: (microplastic(s) OR plastic debris OR nanoplastic(s)) AND (aggregation OR agglomeration OR flocculation OR coagulation OR incorporation OR aggregate(s) OR floc(s) OR agglomerate(s)). A total of 2,407 articles related to these search terms were found. We filtered this list based on our specific research question, such that relevant articles should (1) include information relating to plastics and MPs, (2) relate to the flocculation

processes of MPs in aquatic environments and (3) be peer-reviewed, original research articles. After applying these criteria, 117 articles remained. Of these remaining papers, only those that reported (1) the size and shape of MPs and (2) the size of aggregates were considered for analysis in this Article. As this study focused on how MPs interact with SPM through flocculation in the water column, processes such as the biological passage of MPs from uptake to excretion, leading to the formation of faecal pellets that contain MPs, were not covered in this investigation.

Data collection. From this final corpus of papers, details of the MPs and flocculation process were systematically compiled (Supplementary Data 1). The MPs in the flocculation experiments were first categorized into three distinct shapes: microspheres (perfect spherical shape), fragments (irregular shape degraded from large plastic pieces) and microfibrils (elongated shape shed from textile materials such as clothes, masks and fishing tools). The size of the MPs was also recorded, including the diameter of microspheres and the diameter and length of microfibrils. For fragments, the longest and shortest axes were recorded, but it was noted that some of the studies lacked either the shortest or the longest axis length. Furthermore, the long and short dimensions were analysed using the aspect ratio (AR). When the AR was not available, nominal ARs of 1.5 for particle-shaped fragments and 3.0 for fibre-shaped fragments were assigned⁴⁸. The upper and lower limits of the size range, together with the median/mean size, were recorded (depending on their availability). Moreover, the polymer type, weathering condition, density and surface roughness of the MPs were also collated for analysis, to indicate how these parameters influence and contribute towards flocculation.

Flocculation data were collected simultaneously and subsequently paired with the respective MP characteristics. The size of flocs with a solitary characteristic dimension (that is, longest axis) was collected because this is the classic method to characterize flocs²⁹. The floc data were sorted in terms of the lower limit, mean/medium and upper limit, each depending on data availability. The mean or medium size of flocs was used to analyse their relationship with MPs, and the lower- and upper-bound were also included depending on data availability. The environmental conditions for generating flocs were also recorded, including hydrodynamics, SPM type and concentration, salinity, and organic and inorganic matter (as these can enhance flocculation during experiments). The acquisition domains were then classified into six categories: marine, freshwater, estuary, lake and reservoir, river and water treatment plants, each according to their environmental conditions and floc type.

The efficiency of MP incorporation into flocs was recorded and expressed in terms of the incorporation rate, which is the ratio between incorporated MPs and total MPs. If the incorporation rate was below 10%, the MPs were considered as unincorporated. If the incorporation rate was in the range of 10–40% for one type of MP, the lower limit of the MP size range was recorded as incorporated. If the incorporation rate was between 40% and 80%, the lower limit and mean/medium were recorded as incorporated. If the incorporation rate was >80%, all sizes (lower limit, mean/medium and upper limit) were acknowledged as being incorporated. Quantitative data were not available for some studies and only the qualitative data were collected. In these cases, the incorporation rate was nominally classified as Low, Medium or High (according to the narrative description). Both incorporated and unincorporated MPs were compiled and analysed. Some data were not available in the text and tables of main articles and so the data were directly acquired by digitally re-measuring figures in the original articles that illustrated incorporated MPs within the respective flocs, initially using ImageJ software. The figures were then further assessed for MP and floc size using WebPlotDigitizer (version 4.6). To maintain consistency, the data collection protocols employed for the other datasets were observed in the redigitized data acquisition.

Data analysis. A total of 2,580 measurements were compiled from 28 scientific articles (Supplementary Data 1). The size relationships between MPs and flocs were plotted in Fig. 2 using Matplotlib (3.3.4) in Python (3.6.4). The boundary curve between incorporated MPs and unincorporated MPs was derived from quantile regression of the incorporated MPs.

Laboratory flocculation experiments

Materials. MPs were selected on the basis of the meta-analysis (Fig. 2). Three shapes of MPs (microspheres, fragments and microfibrils) with wide size ranges were used in the flocculation experiments. Due to the extensive studies previously conducted on microspheres, only PE microspheres (Cospheric) with a size range of 10–150 μm were included in these experiments. Microspheres were weathered using ultraviolet (UV) light to assess the influence of MP ageing on the flocculation process. In the case of fragments, previous studies tended to use limited size ranges and polymer types to study the flocculation of fragment MPs, even though fragments are regarded as the most dominant and environmentally important MPs in the natural environment. Five polymer types (PE, PP, PS, PET and PVC) with various fragment densities were used (Supplementary Text 1). Their sizes were in the range of 10–250 μm , which is in the size range of the boundary curve determined from the meta-analysis. The characteristics of various MPs are presented in Supplementary Tables 1 and 2. Microfibrils are the most detectable MPs found in the natural environment^{21,48}, but the study of their flocculation behaviour is quite limited^{11,19}. Previous studies mostly focused on the length of MPs or the different behaviours of microfibrils compared with fragments and microspheres, but there have been no studies that systematically examined the flocculation of microfibrils². Therefore, a wide range of microfibrils of different textile materials were included. These ranged from N95 masks, clothes, cigarette filter, carpet, ropes and duvet filling. The fibre diameters spanned $9.77 \pm 0.71 \mu\text{m}$ to $48.90 \pm 3.33 \mu\text{m}$ with lengths ranging from below 10 μm to over 2,000 μm (Supplementary Table 1) and comprised five polymer classifications (PP, PET, polyamide/nylon, acrylic and cellulose acetate) and three density types (low, medium and high density relative to the density of seawater).

To study the influence of weathering on flocculation, six types of MP (PE microspheres and fragments, PP fragments, and three PP microfibrils with different diameters and textures), together with a full size range of pristine MPs, were selected. The MPs were weathered using UV light (Vilber Lourmat TFX-35 MC UV lamp) for 3 days (Supplementary Text 2). The weathered MPs are deemed to more closely resemble the MPs originating from the natural environment^{27,45}. It should be noted that the weathering process changed only the surface chemistry and not the physical parameters, such as size and surface roughness. This enabled us control a single variable to gauge the influence of weathering. In total, 20 types of MP with different size ranges were included in this Article to investigate the influence of MP properties on flocculation and also to validate the results of the meta-analysis (detailed information on the MPs are presented in Supplementary Tables 1 and 2). Non-fluorescent MPs were dyed with Nile Red to distinguish MPs from the encapsulating flocs by fluorescence microscopy¹¹ (Supplementary Text 3).

Bentonite (Sigma-Aldrich, 285234), a commonly used artificial clay mineral sediment⁴⁹, was used in this Article as SPM at a concentration of 250 mg l^{-1} , which is in the range of estuarine turbidity maxima concentrations^{28,33}. Xanthan gum (Sigma-Aldrich, G1253) is a proxy for the natural exopolymer secreted by microorganisms, often referred to as EPS, and is widely used as EPS in flocculation experiments⁴⁹. The concentration of xanthan gum was set at 4% of the sediment, at 10 mg l^{-1} , which is in the region of organic concentrations typically found in estuaries⁵⁰. Artificial seawater was made from artificial sea salt (Sigma-Aldrich, S9883) by dissolving 34 g artificial sea salt in 1 l deionized water.

One millimetre of 10 mg l⁻¹ fluorescently labelled MPs was characterized using a Leica DMIL inverted microscope with a Leica EL 6000 fluorescent light source and pictured using a Leica DFC420 C colour camera. The digital images contained 1,360 × 1,024 pixels with a pixel size of 1.095 μm² and were used to characterize the size distribution and shape of the MPs. The captured images were processed using ImageJ software (Fiji, Version 2.0) to determine the size distribution of the MPs. The surface morphology of the MPs was also analysed by scanning electron microscopy (FEI Inspect-F; Supplementary Table 2). The size distribution of bentonite was determined using a Beckman Coulter laser granulometer.

Flocculation experiments. The suspended sediment (250 mg l⁻¹), xanthan gum (10 mg l⁻¹) and each type of MP (10 mg l⁻¹) were added to roller bottles (400 ml). Each roller bottle was filled with artificial seawater and then immersed in an ultrasonic water bath for 15 min to break up the preformed flocs. Each roller bottle was then rolled on a roller table for 2 h (Thermo Scientific Roller) at a rotational speed of 25 rpm. The hydrodynamic conditions were close to those typically observed in low hydrodynamic estuarial and ocean surface water column conditions¹¹ (Supplementary Text 4). After rolling, a modified wide pipette (6 mm)^{30,33} was used to promptly sample the suspension (2 ml, midpoint of the roller bottle). The sampled suspension was carefully and evenly deposited into a Petri dish. Each sample contained 30 drops of suspension and were observed with an inverted fluorescence microscope with an objective of ×100 and digitally imaged. Each MP was observed and recorded, and 100–300 digital stills were taken (the frequency was dependent on the type of MP). The experiments were performed in triplicate for each MP type.

The influence of Nile Red on the flocculation characteristics was evaluated using PET and PP fibres. We found that there was no difference between dyed and pristine MPs regarding incorporation rate. Different sampling volumes were also tested (2, 5 and 10 ml); we found that 2 ml was sufficient to identify the status of the MPs (incorporated and unincorporated). A sampling volume of 2 ml included over 200 MPs, which was deemed sufficient data to rigorously analyse the flocculation behaviour of MPs.

Data processing and analysis. The raw pictures were imported into ImageJ (Fiji, Version 2.0) and the MP status (incorporated and unincorporated) was recorded, together with the measured size of the MPs (diameter for microspheres, length for microfibrils, and Feret and MinFeret diameters for fragments). The incorporation rate was calculated as the ratio between incorporated MPs and the total MPs in each size range of MPs. The sizes of the incorporated MPs and hosting flocs were measured manually to analyse the size relationships. The size relationships between MPs and flocs are plotted in Fig. 3. The ratios of incorporated MPs below or above the boundary curve derived from the meta-analysis were used to assess the robustness of the boundary curve. The incorporation rate of MPs with different sizes and properties was also used to compare the boundary size from meta-analysis.

Data availability

All data files in .xlsx format are available as Supplementary Data 1 and 2.

Code availability

The code for plotting the figures is available via Figshare at <https://doi.org/10.6084/m9.figshare.27119601> (ref. 51).

References

- Isobe, A., Iwasaki, S., Uchida, K. & Tokai, T. Abundance of non-conservative microplastics in the upper ocean from 1957 to 2066. *Nat. Commun.* **10**, 417 (2019).
- Koelmans, A. A. et al. Risk assessment of microplastic particles. *Nat. Rev. Mater.* **7**, 138–152 (2022).
- Brandon, J. A., Jones, W. & Ohman, M. D. Multidecadal increase in plastic particles in coastal ocean sediments. *Sci. Adv.* **5**, eaax0587 (2019).
- Thompson, R. C. et al. Lost at sea: where is all the plastic?. *Science* **304**, 838 (2004).
- Droppo, I. G. Rethinking what constitutes suspended sediment. *Hydrol. Process.* **15**, 1551–1564 (2001).
- Smoczyński, L. et al. Modelling the structure of sludge aggregates. *Environ. Technol.* **37**, 1122–1132 (2016).
- Spencer, K. L. et al. A structure–function based approach to floc hierarchy and evidence for the non-fractal nature of natural sediment flocs. *Sci. Rep.* **11**, 14012 (2021).
- Turner, J. T. Zooplankton fecal pellets, marine snow, phytodetritus and the ocean's biological pump. *Prog. Oceanogr.* **130**, 205–248 (2015).
- Leiser, R. et al. Interaction of cyanobacteria with calcium facilitates the sedimentation of microplastics in a eutrophic reservoir. *Water Res.* **189**, 116582 (2021).
- Yang, X., An, C., Feng, Q., Boufadel, M. & Ji, W. Aggregation of microplastics and clay particles in the nearshore environment: characteristics, influencing factors, and implications. *Water Res.* **224**, 119077 (2022).
- Porter, A., Lyons, B. P., Galloway, T. S. & Lewis, C. Role of marine snows in microplastic fate and bioavailability. *Environ. Sci. Technol.* **52**, 7111–7119 (2018).
- Leiser, R., Schumann, M., Dadi, T. & Wendt-Potthoff, K. Burial of microplastics in freshwater sediments facilitated by iron–organo flocs. *Sci. Rep.* **11**, 24072 (2021).
- Möhlenkamp, P., Purser, A. & Thomsen, L. Plastic microbeads from cosmetic products: an experimental study of their hydrodynamic behaviour, vertical transport and resuspension in phytoplankton and sediment aggregates. *Elementa* **6**, 61 (2018).
- Bergmann, M. et al. High quantities of microplastic in Arctic deep-sea sediments from the HAUSGARTEN observatory. *Environ. Sci. Technol.* **51**, 11000–11010 (2017).
- Zhao, S., Mincer, T. J., Lebreton, L. & Egger, M. Pelagic microplastics in the North Pacific Subtropical Gyre: a prevalent anthropogenic component of the particulate organic carbon pool. *PNAS Nexus* <https://doi.org/10.1093/pnasnexus/pgad070> (2023).
- Bergmann, M., Allen, S., Krumpfen, T. & Allen, D. High levels of microplastics in the Arctic sea ice alga *Melosira arctica*, a vector to ice-associated and benthic food webs. *Environ. Sci. Technol.* <https://doi.org/10.1021/acs.est.2c08010> (2023).
- Besseling, E., Quik, J. T. K., Sun, M. & Koelmans, A. A. Fate of nano- and microplastic in freshwater systems: a modeling study. *Environ. Pollut.* **220**, 540–548 (2017).
- Andersen, T. J., Rominikan, S., Olsen, I. S., Skinnebach, K. H. & Fruergaard, M. Flocculation of PVC microplastic and fine-grained cohesive sediment at environmentally realistic concentrations. *Biol. Bull.* **240**, 42–51 (2021).
- Lapointe, M., Farner, J. M., Hernandez, L. M. & Tufenkji, N. Understanding and improving microplastic removal during water treatment: impact of coagulation and flocculation. *Environ. Sci. Technol.* **54**, 8719–8727 (2020).
- Onink, V., Kaandorp, M. L. A., van Sebille, E. & Laufkötter, C. Influence of particle size and fragmentation on large-scale microplastic transport in the Mediterranean Sea. *Environ. Sci. Technol.* <https://doi.org/10.1021/acs.est.2c03363> (2022).
- Waldschläger, K. et al. Learning from natural sediments to tackle microplastics challenges: a multidisciplinary perspective. *Earth Sci. Rev.* **228**, 104021 (2022).
- Kvale, K., Prowe, A. E. F., Chien, C.-T., Landolfi, A. & Oschlies, A. The global biological microplastic particle sink. *Sci. Rep.* **10**, 16670 (2020).

23. Lobelle, D. et al. Global modeled sinking characteristics of biofouled microplastic. *J. Geophys. Res. Oceans* **126**, e2020JC017098 (2021).
24. Long, M. et al. Interactions between microplastics and phytoplankton aggregates: impact on their respective fates. *Mar. Chem.* **175**, 39–46 (2015).
25. Ho, Q. N., Fettweis, M., Spencer, K. L. & Lee, B. J. Flocculation with heterogeneous composition in water environments: a review. *Water Res.* <https://doi.org/10.1016/j.watres.2022.118147> (2022).
26. Li, Y. et al. Interactions between nano/micro plastics and suspended sediment in water: implications on aggregation and settling. *Water Res.* **161**, 486–495 (2019).
27. Lebreton, L., Egger, M. & Slat, B. A global mass budget for positively buoyant macroplastic debris in the ocean. *Sci. Rep.* **9**, 12922 (2019).
28. Tran, D. & Strom, K. Suspended clays and silts: are they independent or dependent fractions when it comes to settling in a turbulent suspension? *Cont. Shelf Res.* **138**, 81–94 (2017).
29. Thomas, D. N., Judd, S. J. & Fawcett, N. Flocculation modelling: a review. *Water Res.* **33**, 1579–1592 (1999).
30. Lapointe, M. & Barbeau, B. Characterization of ballasted flocs in water treatment using microscopy. *Water Res.* **90**, 119–127 (2016).
31. Shen, X., Lee, B. J., Fettweis, M. & Toorman, E. A. A tri-modal flocculation model coupled with TELEMAC for estuarine muds both in the laboratory and in the field. *Water Res.* **145**, 473–486 (2018).
32. Lee, B. J., Fettweis, M., Toorman, E. & Molz, F. J. Multimodality of a particle size distribution of cohesive suspended particulate matters in a coastal zone. *J. Geophys. Res. Oceans* **117**, C03014 (2012).
33. Manning, A. J. & Schoellhamer, D. H. Factors controlling floc settling velocity along a longitudinal estuarine transect. *Mar. Geol.* **345**, 266–280 (2013).
34. Kolmogorov, A. N. The local structure of turbulence in incompressible viscous fluid for very large Reynolds numbers. *Proc. R. Soc. A* **434**, 9–13 (1991).
35. Zhao, S., Ward, J. E., Danley, M. & Mincer, T. J. Field-based evidence for microplastic in marine aggregates and mussels: implications for trophic transfer. *Environ. Sci. Technol.* **52**, 11038–11048 (2018).
36. Galgani, L. et al. Hitchhiking into the deep: how microplastic particles are exported through the biological carbon pump in the North Atlantic Ocean. *Environ. Sci. Technol.* <https://doi.org/10.1021/acs.est.2c04712> (2022).
37. Tekman, M. B. et al. Tying up loose ends of microplastic pollution in the Arctic: distribution from the sea surface through the water column to deep-sea sediments at the HAUSGARTEN observatory. *Environ. Sci. Technol.* **54**, 4079–4090 (2020).
38. Roscher, L. et al. Microplastic pollution in the Weser estuary and the German North Sea. *Environ. Pollut.* **288**, 117681 (2021).
39. Sun, X. et al. Factors influencing the occurrence and distribution of microplastics in coastal sediments: from source to sink. *J. Hazard. Mater.* **410**, 124982 (2021).
40. Zhang, M., Xu, D., Liu, L., Wei, Y. & Gao, B. Vertical differentiation of microplastics influenced by thermal stratification in a deep reservoir. *Environ. Sci. Technol.* <https://doi.org/10.1021/acs.est.2c09448> (2023).
41. Lapointe, M., Jahandideh, H., Farner, J. M. & Tufenkji, N. Super-bridging fibrous materials for water treatment. *npj Clean Water* **5**, 11 (2022).
42. van Sebille, E. et al. A global inventory of small floating plastic debris. *Environ. Res. Lett.* **10**, 124006 (2015).
43. Cole, M. et al. Microplastics alter the properties and sinking rates of zooplankton faecal pellets. *Environ. Sci. Technol.* **50**, 3239–3246 (2016).
44. Jåms, I. B., Windsor, F. M., Poudevigne-Durance, T., Ormerod, S. J. & Durance, I. Estimating the size distribution of plastics ingested by animals. *Nat. Commun.* **11**, 1594 (2020).
45. MacLeod, M., Arp, H. P. H., Tekman, M. B. & Jahnke, A. The global threat from plastic pollution. *Science* **373**, 61–65 (2021).
46. Bergami, E. et al. Long-term toxicity of surface-charged polystyrene nanoplastics to marine planktonic species *Dunaliella tertiolecta* and *Artemia franciscana*. *Aquat. Toxicol.* **189**, 159–169 (2017).
47. Baekeland, L. H. Method of making insoluble products of phenol and formaldehyde. *U.S. Patent* **942**, 699 (1909).
48. Kooi, M. et al. Characterizing the multidimensionality of microplastics across environmental compartments. *Water Res.* **202**, 117429 (2021).
49. Spencer, K. L. et al. Quantification of 3-dimensional structure and properties of flocculated natural suspended sediment. *Water Res.* **222**, 118835 (2022).
50. Morelle, J., Schapira, M. & Claquin, P. Dynamics of phytoplankton productivity and exopolysaccharides (EPS and TEP) pools in the Seine Estuary (France, Normandy) over tidal cycles and over two contrasting seasons. *Mar. Environ. Res.* **131**, 162–176 (2017).
51. Wu, N., Grieve, S. W. D., Manning, A. J. & Spencer, K. L. Flocs as vectors for microplastics in the aquatic environment. *Figshare* <https://doi.org/10.6084/m9.figshare.27119601> (2024).

Acknowledgements

This project was supported by Lloyd's Register Foundation, UK, Queen Mary University of London Principal Studentships and EU INTERREG France (Channel) England project 'Preventing Plastic Pollution' co-financed by the European Regional Development Fund. A.J.M.'s contribution to this research was also partly supported by the US National Science Foundation under grants OCE-1736668 and OCE-1924532, TKI-MUSA Project 11204950-000-ZKS-0002 and the HR Wallingford Company Research projects 'FineScale' (ACK3013_62) and 'Support for QMUL Floc Research' (DDY0524). We also thank technical staff at the School of Geography and School of Biological and Behavioural Sciences at Queen Mary University of London and J. Ming at Queen Mary University of London for characterizing microplastic samples by scanning electron microscopy.

Author contributions

Conceptualization: N.W., S.W.D.G., A.J.M. and K.L.S. Methodology: N.W., S.W.D.G., A.J.M. and K.L.S. Investigation: N.W. and K.L.S. Visualization: N.W., S.W.D.G., A.J.M. and K.L.S. Funding acquisition: K.L.S. and A.J.M. Project administration: S.W.D.G. and K.L.S. Supervision: S.W.D.G., A.J.M. and K.L.S. Writing—original draft: N.W. and K.L.S. Writing—review and editing: N.W., S.W.D.G., A.J.M. and K.L.S.

Competing interests

The authors declare no competing interests.

Additional information

Supplementary information The online version contains supplementary material available at <https://doi.org/10.1038/s44221-024-00332-4>.

Correspondence and requests for materials should be addressed to Nan Wu.

Peer review information *Nature Water* thanks Michael Bank and the other, anonymous, reviewer(s) for their contribution to the peer review of this work.

Reprints and permissions information is available at www.nature.com/reprints.

Publisher's note Springer Nature remains neutral with regard to jurisdictional claims in published maps and institutional affiliations.

Open Access This article is licensed under a Creative Commons Attribution 4.0 International License, which permits use, sharing, adaptation, distribution and reproduction in any medium or format, as long as you give appropriate credit to the original author(s) and the source, provide a link to the Creative Commons licence, and indicate if changes were made. The images or other third party material in this

article are included in the article's Creative Commons licence, unless indicated otherwise in a credit line to the material. If material is not included in the article's Creative Commons licence and your intended use is not permitted by statutory regulation or exceeds the permitted use, you will need to obtain permission directly from the copyright holder. To view a copy of this licence, visit <http://creativecommons.org/licenses/by/4.0/>.

© The Author(s) 2024